Calculating human thermal comfort and thermal stress in the PALM model system 6.0

Fröhlich Dominik[1] and Matzarakis Andreas[1]

[1]Deutscher Wetterdienst (DWD), Research Centre Human Biometeorology, Stefan-Meier-Str. 4, 79104 Freiburg

Correspondence: Dominik Fröhlich (dominik.froehlich@mailbox.org)

Abstract. In the frame of the project "MOSAIK – Model–based city planning and application in climate change", a German-wide research project within the call "Urban Climate Under Change" ($[\mathrm{UC}]^2$) funded by the German Federal Ministry of Education and Research (BMBF), a biometeorology module was implemented into the PALM model system. The new biometeorology module comprises of methods for the calculation of uv-exposure quantities, a human–biometeorologically weighted mean radiant temperature ($\mathrm{T_{mrt}}$), as well as for the estimation of human thermal comfort or stress. The latter is achieved through the implementation of the three widely–used thermal indices Perceived Temperature (PT), Universal Thermal Climate Index (UTCI), as well as Physiologically Equivalent Temperature (PET) together with a newly developed instationary index instationary Perceived Temperature (iPT) based on PT for use with the multi–agent model. Comparison calculations were performed for the indices PT, UTCI and PET based on the SkyHelios model and showing PALM calculates higher values in general. This is mostly due to a higher radiational gain leading to higher values of mean radiant temperature. For a more direct comparison, the indices PT, PET and UTCI were calculated by the biometeorology module, as well as the programs provided by the attachment to the VDI guideline 3787, as well as by the RayMan model based on the very same input dataset. Results show deviations below the relevant precision of 0.1 K for PET and UTCI and some deviations of up to 2.683 K for PT caused by repeated unvaovourable rounding in very rare cases (0.027 %).

1 Introduction

Urban areas show slightly different diurnal variability in air temperature ($\mathrm{T_a}$) compared to their surroundings (e.g. Oke, 1995; Helbig et al., 1999). This is mostly due to modifications in the radiation budget caused by ground sealing, different surface materials and many vertical surfaces (Oke, 1995, p. 276ff). Additionally many of them have high heat storage capacities (Oke, 1995, p. 284) reducing night–time cooling. The two effects contribute to a phenomenon that is called the Urban Heat Island (UHI, Oke, 1995, p. 288ff). Another increase in urban temperatures is caused by the local impact of global climate change. E.g. for Freiburg (south–west Germany), an increase of days with heat stress by up to 5 % is expected (Matzarakis and Endler, 2010).

Health and well–being of the growing urban population is already an important issue in present urban planning (e.g. Helbig et al., 1999). A number of studies have been carried out in the last years that show strong correlation between health, as well as mortality on the one side and urban biometeorology on the other side. Especially heat stress during the summer months seems to lead to an increase in mortality (e.g. Koppe et al., 2004; Conti et al., 2005; Muthers et al., 2010; Nastos and Matzarakis, 2012; Muthers et al., 2017).

To allow for counteracting malicious effects through urban planning meassures, e.g. by a modification in the building configuration (Lin et al., 2010a), surface materials (Lin et al., 2010b) or urban green (Shashua-Bar et al., 2011; Charalampopoulos et al., 2015) decision makers are dependent on spatially resolved thermal perception information that can be best provided through maps (Matzarakis, 2001; Nouri et al., 2018).

Thermal comfort can be assessed by calculating thermal indices, e.g. the Predicted Mean Vote (PMV Fanger, 1972), Physiologically Equivalent Temperature (PET, Höppe, 1993, 1999), the Perceived Temperature (PT, Staiger et al., 2012) or the Universal Thermal Climate Index (UTCI, Jendritzky et al., 2012) combining several aspects to approximate the thermal perception of a standardized sample human being taking into account many meteorological and physiological parameters (Fanger, 1972; Höppe, 1999; Staiger et al., 2012, 2019).

To facilitate the identification of hotspots and the assessment of potential for the reduction of thermal stress the program "Urban Climate Under Change" ($[\mathrm{UC}]^2$) is funded by the German Federal Ministry of Education and Research (BMBF). It "aims at the development, validation and application of an innovative urban climate model for entire cities" (Todo: UC2 homepage). Part of the $[\mathrm{UC}]^2$ program is the German-wide research project "MOSAIK – Model–based city planning and application in climate change". In the course of MOSAIK the PALM (PArallelized Large–eddy simulation Model Raasch and Schröter, 2001; Maronga et al., 2015; Hellsten et al., 2018; Maronga et al., 2019b) is extended by several modules to extend it to become a comprehensive urban climate model (e.g. an urban surface module by Resler et al. (2017)). One of the new modules is the biometeorology module capable of calculating the static thermal indices PT, UTCI and PET as well as the instationary index "instationary Perceived Temperature" (iPT) for use with the PALM multi–agent model (Maronga et al., 2019b).

2 Methods

Humans are unable to directly sense individual meteorological quantities, e.g. $\mathrm{T_a}$. However, they do feel the thermal effect of their environment caused by several meteorological parameters integrally through the skin and the blood temperature in the thermoregulatory system of the hypothalamus (Tromp, 1980; Höppe, 1993). Thermal comfort therefore can not be described by individual parameters, but needs to be approximated through thermal comfort indices considering all relevant conditions. The more sophisticated indices are based on the approach of equivalent temperaturs and are relying on the evaluation of the human energy balance or heat flux models (e.g. Fanger, 1972; Gagge et al., 1986; Höppe, 1993; Błażejczyk et al., 2012).

An important input parameter to all sophisticated thermal indices is the mean radiant temperature ($\mathrm{T_{mrt}}$), defined as the temperature of a perfectly black environment causing thermal radiation only, that leads to the same radiational gain or loss than the actual environment (Fanger, 1972).

The estimation of $\mathrm{T_{mrt}}$ does require radiational input data, that is provided by one of the two radiation schemes available in PALM, the simple clear-sky model (Maronga et al., 2019a), or the more complex RRTMG (Mlawer et al., 1997; Pincus et al., 2003; Maronga et al., 2019a).

2.1 Perceived Temperature

The Perceived Temperature (PT) is a thermal comfort index for outdoor environments using the concept of an equivalent temperature. The thermal impact of the environment is evaluated through the "Klima–Michel–Model" (Jendritzky et al., 1990), an energy balance model for human beings (Staiger et al., 2012). PT is defined to be "the air temperature of a reference environment in which the thermal perception would be the same as in the actual environment" (Staiger et al., 2012).

PT is a steady–state model by design to keep run–time at a reasonable level. The target for PT is a standardized sample human (the "Klima–Michel", Jendritzky et al., 1990) with a height of 1,75 m, an age of 35 years, a weight of 75 kg, an internal heat production of 135 W/m² walking at a speed of 4 km/h (Staiger et al., 2012). This allows for a simplification of the human heat balance equation after ASHRAE (2001, p. 134):

$$M - Wo = (C + R + E_{sk}) + (C_{res} + E_{res}) + S_{sk} + S_{cr} \tag{1}$$

The energy gain caused by metabolic processes within the body M reduced by the portion of mechanical work Wo (the fraction of the body's energy, that is not converted to heat, but to mechanical workforce) is compared to the combined latent and sensible heat fluxes from or to the environment. The components of the equation represent energy transfer by sensible heat C, radiation R, and latent heat E. Eq. 1 distinguishes between fluxes from or to the skin ($_{sk}$), the core ($_{cr}$) and through the respiratory system ($_{res}$). The heat storage components (S) are considered to equal 0 W constantly assuming a steady–state. Unit of all parameters is W.

All of the physiological parameters are defined by the "Klima–Michel" model and the clothing model is self-adapting. PT can therefore be estimated exclusively based on the meteorological parameters air temperature ($\mathrm{T_a}$, °C), wind speed(v, m/s), vapor pressure (VP, hPa), and mean radiant temperature ($\mathrm{T_{mrt}}$, °C). All of the energy gained or lost by the "Klima-Michel" is compared to that of an "indoor" reference environment (compare to Figure 1). This is done based on a modified version of the basic thermal index "Predicted Mean Vote" (PMV) after Fanger (1972); Gagge et al. (1986). The reference environment is defined with parameters $\mathrm{T_{mrt}}$ = $\mathrm{T_a}$ (no radiational impact), v = 0.1 m/s (auto-convection only) and VP equal to VP of the actual environment. If the actual environment would lead to warm and humid conditions, VP is set to a value matching a relative humidity of 50 % (Staiger et al., 2012). The comparison is balanced by the air temperature of the "indoor" environment that is modified until the thermal stress in terms of PMV is the same as in the actual environment.

The index PMV does consider energy exchange based on a two-node body model (a skin and a core node). It allows for latent and sensible heat transfer from or to the skin (considering sweating) and by respiration (Fanger, 1972; Staiger et al., 2012).

PT comprises a clothing model, that is automatically selecting the most appropriate value for the clothing index (clo) according to the prevailing meteorological conditions (Staiger et al., 2012). It primarily attempts to maintain thermal comfort by adapting

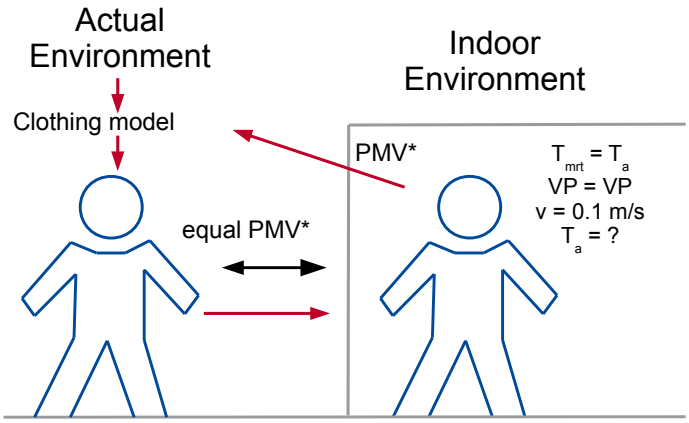

Figure 1. Schematic overview of the comparison of adjusted PMV between the actual prevailing environment and a virtual eindoor environment for the estimation of the perceived temperature. The sample human is standardized by the "Klima–Michel" model.

to hot or cold conditions. Only if this can not be achieved, thermal stress is computed (Fanger, 1972; Staiger et al., 2012). The clothing model is supported in reducing thermal strain by parametrizations of shivering in cold conditions (PMV < -0.11 at clo = 1.75) and sweating under hot conditions (PMV > 0.5 at clo = 0.5, Staiger et al., 2012).

Table 1. The thermo-physiological meaning of PT results for central Europe as defined by Staiger et al. (2012).

PT (°C)	Thermal Perception	Thermo-physiological stress
≥ +38	Very hot	Extreme heat stress
+32 – +38	Hot	Great heat stress
+26 – +32	Warm	Moderate heat stress
+20 – +26	Slightly warm	Slight heat stress
0 – +20	Comfortable	Comfort possible
-13 – 0	Slightly cool	Slight cold stress
-26 – -13	Cool	Moderate cold stress
-39 – -26	Cold	Great cold stress
< -39	Very cold	Extreme cold stress

To facilitate the interpretation of PT results in Central Europe Staiger et al. (2012) published a perception table translating the PT values into thermal perception or the extent of thermo-physiological stress (Table 1).

2.1.1 Universal Thermal Climate Index

The Universal Thermal Climate Index (UTCI) is "the isothermal air temperature of the reference condition that would elicit in the same dynamic response (strain) of the physiological model" than the actual environment Jendritzky et al. (2012)

Alike most complex thermal indices (e.g. PT or PET), UTCI is an equivalent temperature. The thermal effect of the prevailing meteorological conditions is compared to the one of a standardized reference "indoor" environment with a fix 50 % relative humidity, calm air (0.1 m/s) and T_{mrt} equal to T_a (Jendritzky et al., 2012). The environments are compared by a heat transfer model introduced by Fiala et al. (2012).

For performance reasons, UTCI can only be approximated using a regression equation abbreviated from sample calculations performed by computing centers (Jendritzky et al., 2012; Bröde et al., 2012). It allows for a computationally cheap and highly performant determination of UTCI. However, it also causes a limited range of input parameters it can deal with. The regression equation supports T_a in the range of -50.0°C to +50.0°C, a relative humidity from 0 % to 100 %, wind speed of at least 0.5 m/s and up to 17.0 m/s, as well as a difference between T_{mrt} and T_a (T_{mrt} - T_a) of -30.0°C to +70.0 °C. In case the local meteorological conditions are out of bounds, specific workarounds after Bröde et al. (2012) can be implemented.

Due to the evaluation by the regression equation, physiological parameters can not be modified in UTCI and are considered to be static. UTCI does assume a permanent walking speed of 4 km/h (1.11 m/s) resulting in an internal heat production of 135 W/m² (Jendritzky et al., 2012) and the clothing insulation to be self-adapting according to the environmental conditions (Havenith et al., 2012).

As long as all input conditions are in range for the regression equation UTCI is quite sensitive to wind speed (Chen and Matzarakis, 2018; Fröhlich and Matzarakis, 2016), but also to T_a and T_{mrt} (Chen and Matzarakis, 2018; Fröhlich and Matzarakis, 2016).

Table 2. Thermal stress classification for UTCI. Modified after Błażejczyk et al. (2013).

UTCI (°C)	Thermal Stress category
$\geq$ +46	Extreme heat stress
+38 – +46	Very strong heat stress
+32 – +38	Strong heat stress
+26 – +32	Moderate heat stress
+9 – +26	No thermal stress
0 – +9	Slight cold stress
-13 – 0	Moderate cold stress
-27 – -13	Strong cold stress
-40 – -27	Very strong cold stress
$<$ -40	Extreme cold stress

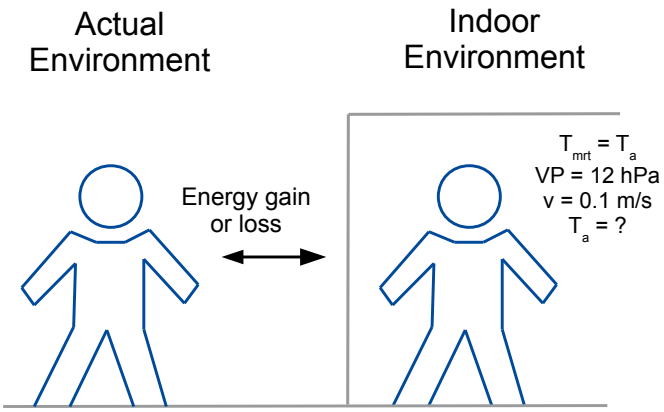

Figure 2. Schematic overview of the comparison of the energy gain or loss in the heat ballance equation between the actual prevailing environment and a virtual eindoor environment for the estimation of the physiologically equivalent temperature. The sample human is represented by the MEMI model.

Błażejczyk et al. (2013) published a thermal stress classification for Central Europe allowing for the interpretation of UTCI results (2). In contrast to the assessment tables for PT (1) and PET (e.g. 3), the UTCI assessment table is a thermal stress classification (Błażejczyk et al., 2013) rather than a thermal comfort evaluation.

2.1.2 Physiologically Equivalent Temperature

The Physiological Equivalent Temperature (PET) can be considered to be one of the most popular thermal index and is widely used for the assessment of human thermal comfort. Höppe (1999) defiens PET as "the air temperature at which, in a typical indoor setting (without wind and solar radiation), the energy budget of the human body is balanced with the same core and skin temperature as under the complex outdoor conditions to be assessed" (Mayer and Höppe, 1987; Höppe, 1999, compare to Figure 2). PET evaluates heat load based on a simplified human energy balance model by (Höppe, 1984), the "Munich Energy Balance Model for Individuals" (MEMI, Höppe, 1984). PET does not comprise a self-adapting clothing model, but is entirely depending on the user input. It therefore does not include any behavioural components making PET "a real climatic index describing the thermal environment in a thermo-physiologically weighted way" (Höppe, 1999).

PET is very sensitive to the input parameter $\mathrm{T_{mrt}}$ (°C, Charalampopoulos et al., 2013; Chen and Matzarakis, 2018). It does also respond strongly to modifications in wind speed (v) and $\mathrm{T_a}$ (°C). Air humidity in terms od vapour pressure (hPa)must be provided as input, but only shows very weak impact on PET (e.g. Chen and Matzarakis, 2018; Fröhlich and Matzarakis, 2016). The thermal environment is evaluated by the human energy balance equation (2, Höppe, 1999).

$$M + Wo + R + C + E_{sk} + E_{res} + E_{sw} + S = 0 \tag{2}$$

It does consider the metabolic heat production (M), the mechanical workload (Wo), radiational heat flux (R), sensible heat flux (C), as well as latent heat (E). E is thereby separated in the components from or to the skin ($_{sk}$), by sweating ($_{sw}$) and by the respiratory system ($_{res}$). The unit of all components of equation 2 is W. Heat storage (S) must permanently equal 0 W to maintain a steady state.

The energy gain or loss by the prevailing thermal environment is compared to that of an virtual "indoor" environment without radiational impact ($\mathrm{T_{mrt}}$ = $\mathrm{T_a}$), calm air (v = 0.1 m/s), and static humidity in terms of VP = 12 hPa (Höppe, 1999). $\mathrm{T_a}$ of the indoor environment is then modified until the indoor environment is causing the same thermal load than the actual environment. The $\mathrm{T_a}$ of that indoor environment then is returned as PET (Höppe, 1999).

Table 3. Thermal sensation classes for human beings in Central Europe (with an internal heat production of 80 W and a heat transfer resistance of the clothing of 0.9 clo (clothing value)) modified after Matzarakis and Mayer (1996).

PET (°C)	Thermal Perception	Grade of physical stress
>41	Very hot	Extreme heat stress
35 – 41	Hot	Strong heat stress
29 – 35	Warm	Moderate heat stress
23 – 29	Slightly warm	Slight heat stress
18 – 23	Comfortable	No thermal stress
13 – 18	Slightly cool	Slight cold stress
8 – 13	Cool	Moderate cold stress
4 – 8	Cold	Strong cold stress
≤ 4	Very cold	Extreme cold stress

PET results can be interpreted using classification tables for the region in question. For Central Europe a classification with nine classes of thermal perception (3) was introduced by Matzarakis and Mayer (1996).

2.1.3 Instationary Perceived Temperature

An instationary index was developed to assess the thermal perception of the agents generated by PALM's agent module.

The multi-agent-model in PALM is a module sending lagrangian-like particles (agents) through the model domain at runtime. The agents are traveling autonomously from a starting point to a pre-defined destination at runtime while automatically finding their optimal route. On their way, they are exposed to varying meteorological conditions. Steady-state thermal indices, e.g. PT (see Section 2.1) are assuming a long time with constant meteorological conditions for the sample person to adapt to their environment. In the case of PT this is 2 hours (Staiger et al., 2012). The conditions for the agents, however, may be altered with any new model timestep or when the agent has traveled to another grid cell, leading to varying conditions in a time range of fractions of seconds. To consider this high frequency of modified input conditions, a new instationary index had to be devel-

oped.

The new instationary index is intended to be able to cope with a wide range of input conditions to be suitable for the use on the micro scale. At the same time, the results should be generally comparable to those by a well-known steady-state index. While UTCI is too costly, except for the regression equation that is not configurable enough, PET is lacking sensitivity to humidity and clothing insulation. The newly developed instationary index therefore is based on the Perceived Temperature. For simplicity it is called instationary Perceived Temperature (iPT) in this study.

iPT is calculated in two phases. At the first call (when an agent is created) an initialization run is performed. The initialization run is very similar to the steady-state PT as the agent is considered to be adapted to its initial environmental conditions. The initial run is also used to calculate the agents internal heat production. This is necessary, as iPT does allow for setting the agents sex (male or female), age (years), height (m), weight (kg) and mechanical workload (W) to consider a wide range of different agents. However, as the agents are currently not generated with different properties, they default to be standardized "Klima-Michels" (compare to Section 2.1). Another important difference between the initial run and the further timesteps is the decision for a clothing insulation in the initial run, that will be kept for all further timesteps. Every agent therefore does decide for some optimal clothing insulation value (clo) while going outside for the first time and must stick to this decision later on for not having to change repeatedly in less than one second.

Based on the personal properties and the clothing insulation determined in the initial run, for any further call a simplified "cycle" run is performed. This will happen regularly for any new agent-timestep and as soon as an agent moves to another cell (with potentially different meteorological input conditions). In the "cycle" phase, iPT will avoid costly iterations in the clothing model, but will consider two storage fields. The first one will store a fraction of the overhead in the comfort equation representing the core storage (S_{cr} in eq. 1). The other one is used to hold the previous clothing temperature (forcing S_{sk} in eq. 1).

The storage component S_{cr}, of course, must not allow for storage modifications (δ_{S}) of any extent. The heat balance is considered stable after 2 hours according to Staiger et al. (2012). Furthermore, following the logic of conduction, larger difference in temperatures will increase heat exchange and, thus, must also increase δ_{S}. As the temperature difference will become smaller with time (assuming constant conditions) δ_{S} must decrease as well. The factor representing the fraction of the current maximum storage modification to use δ_{Scr} (a fraction of maximum core storage S_{cr}) can therefore be estimated as eq. 3.

$$\delta_{Scr} = 1 - EXP(-1 * (10/t_e) * \delta_t) \tag{3}$$

In eq. 3 the time until equilibrium is reached (s, t_e) is considered to be 2 hours. δ_t does represent the time passed since the last calculation (s). Based on δ_{Scr} the resulting energy balance residual (S_{cr}) at a time t can be estimated by eq. 4 based on S_{cr} from the previous run $t-1$.

$$S_{cr}^{t} = \delta_{Scr} * EB + (1 - \delta_{Scr}) * S_{cr}^{t-1} \tag{4}$$

EB in eq. 4 represents the result for the energy balance without storage at time t.

Another storage needs to be considered for the surface temperature of the clothing. While clothing temperature can adapt way faster than S_{cr}, it must

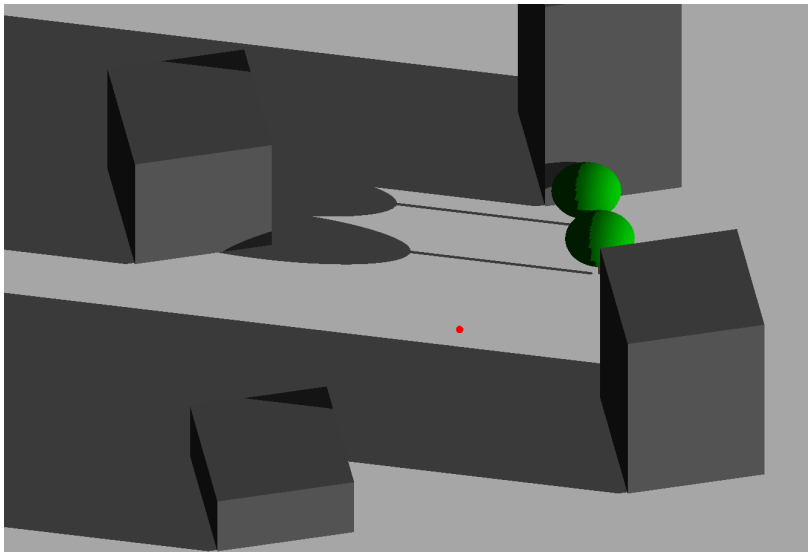

Figure 3. The site "test_urban" with shading as shown by the SkyHelios model seen from South-SouthWest at 07:00 UTC (shortly after sunrise) on a 6$^{\text{th}}$ of March.

2.2 Test case

The thermal comfort part of the biometeorology module was tested based on the generic urban crossroads test–case "test_urban" located at Hannover (Germany) (Fröhlich, 2019, compare to Figure 3). It consists of a 19 x 19 x 60 grid domain with a grid spacing of 2.0 x 2.0 x 2.0 m. In the corners of the domain there are buildings with different heights of 10 m to 40 m. Two streets in between are forming a crossroads. In the North-East of the domain shading is provided by two deciduous trees.
Radiation data for the test case is generated by PALMs clear-sky schmeme providing minimal radiation input based on astronomic calculations assuming a perfectly clear sky without any clouds or obstructions. Please see Section 3.5.1 in Maronga et al. (2019a) for details.

To run the test setup with the thermal comfort part of the biometeorology module, the input file "test_urban_p3d" was slightly modified (Fröhlich, 2019, please see "test_urban_v2.zip/INPUT/test_urban_p3d"). The date was set to the 6$^{\text{th}}$ of March to obtain less extreme conditions. The initial potential temperature was adjusted respectively to better meet typical conditions in March. It was set to 5.0 °C at the surface at startup.

For the assessment of the quality of the results, comparison calculations were performed for 07:00 UTC and 13:00 UTC of a 6$^{\text{th}}$ of March using the well-known and frequently applied SkyHelios model (Fröhlich and Matzarakis, 2018; Fröhlich, 2017; Matzarakis and Matuschek, 2011). Therefore a similar test domain was created for the SkyHelios model (see Figure 3). To increase comparability, the test calculations were driven by the average air temperature calculated by PALM.

2.3 Meteorological Data

For a direct comparison based on the very same input, the thermal indices provided by the biometeorology module were calculated for a meteorological dataset recorded by a urban climate station on top of the chemistry highrise building of the University of Freiburg. The dataset does cover the timespan from 1999-09-01 00:00 LST to 2010-04-30 23:00 LST in 10 minutes resolution and provides the parameters T_a, VP, v and global radiation, that was used to estimate T_{mrt} by the RayMan model. The general statistics of the dataset is provided by Table 4. The output generated by the biometeorology module was then compared to the output by the programs in the attachment to the VDI guideline 3787, part II (VDI, 2008) and to the output by the RayMan model (Matzarakis et al., 2007, 2010).

Table 4. Statistical overview over the meteorological data applied in the comparison of the thermal indices implemented in the biometeorology module to the reference implementations provided by the VDI guideline 3787, part II (VDI, 2008).

	T_a	VP	v	T_{mrt}
Min.	-13.8	-0.8	0.1	-26.0
1st Qu.	6.7	6.3	0.4	0.4
Median	12.7	9.1	0.7	8.7
Mean	12.6	9.7	1.0	11.9
3rd Qu.	18.4	12.5	1.3	19.7
Max.	40.1	43.6	6.2	64.8
NA's	279	2034	15291	17073

3 Results

Results for the test case (e.g. Figures 4 - 6) show the changing thermal conditions over the day. Looking at the perceived temperature (Figure 4) the day starts quite warm with PT of 10.2 to 15.6 °C in the sun and 8.0 to 11.1 °C in shaded areas shortly after sunrise at 07:00 UTC. The differences within the shaded or sunny areas thereby are mostly caused by wind speed. The longwave emissions of the walls, even if they are exposed to direct radiation, what can nicely be seen on the eastern side of the building in the lower left of Figure 4, are weak for surface temperatures are lower than the air temperature. The warm conditions for early spring are caused by a relatively high air temperature of 10.3 - 12.2 °C, that also lead to quite high mean radiant temperature of 11.4 - 14.5 °C in shaded areas and 20.1 - 35.4 °C in the sun. Wind speed is rather low throughout the model domain ranging from less than 0.1 m/s to 0.5 m/s.

The thermo-physiological consequences for a sample human, passing through the model domain are indifferent. According to the thermal perception table for Central Europe, Table 1, all readings are within the class 0 to 20 °C and, thus, can be perceived as comfortable if appropriate clothing is selected. This holds for both, shaded areas, as well as areas exposed to direct radiation.

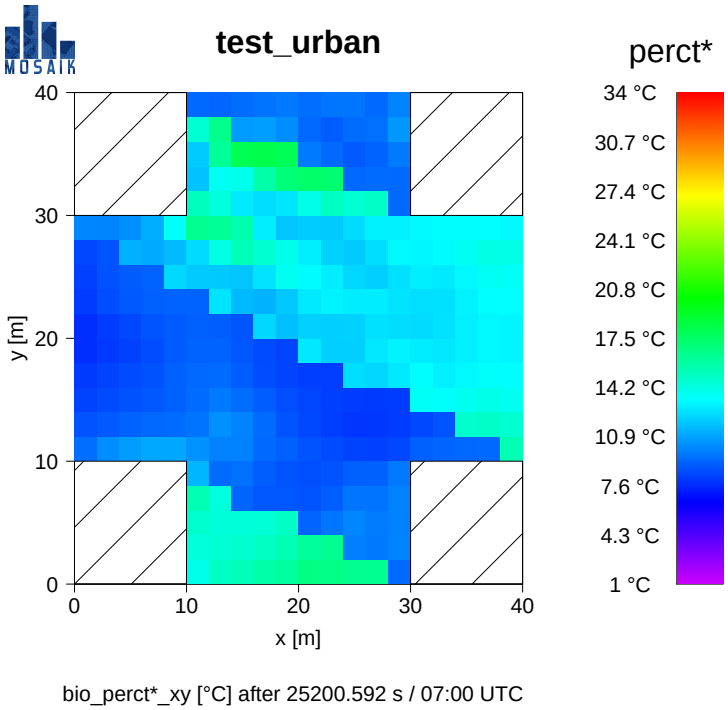

Figure 4. Perceived Temperature (PT, perct* in palm) for the test case "test_urban" at 07:00 UTC (shortly after sunrise) on a 6^{th} of March. Incident wind is from 270° with 1.0 m/s.

The same scenario looks entirely different after midday at 13:00 UTC (see Figure 5). The model's "clear-sky" radiation scheme causes the air temperature to rise to values of 20.8 °C close to the northern wall of the lower right building to 24.3 °C at the western side of the lower right obstacle. Wind speed is little decreased compared to 07:00 and ranges from less than 0.1 m/s to 0.4 m/s at 13:00. Both leads to a quite high mean radiant temperature of 25.7 - 32.7 °C in shaded areas and a very high $\mathrm{T_{mrt}}$ of 44 - 51.7 °C in areas exposed to direct radiation.

A sample human roaming within the model domain would experience wider range of thermal perception. While shaded areas are quite comfortable with PT of 20.0 - 23.4 °C, what translates to "slightly warm" perception according to Table 1, the high $\mathrm{T_{mrt}}$ in unshaded areas also cause high values for PT of 24.4 - 30.9 °C. According to the thermo-physiological perception classification by Staiger et al. (2012, Table 1), the sample person would experience "slightly warm" to "warm" conditions causing slight to moderate heat stress.

The same scenario can also be analyzed targeting thermal stress using the thermal index UTCI (see Section 2.1.1). For 07:00 UTCI calculates quite similar values than PT (compare Figures 4 and 6). The absolute numbers for UTCI are way higher than those for PT with 11.5 - 14.4 °C (UTCI) in the shade and 15.7 - 19.2 °C (UTCI) in sunlit areas. This, however translates to comfortable conditions without thermal stress throughout the entire model domain (compare to Table 2) and therefore is in good agreement with the results for PT.

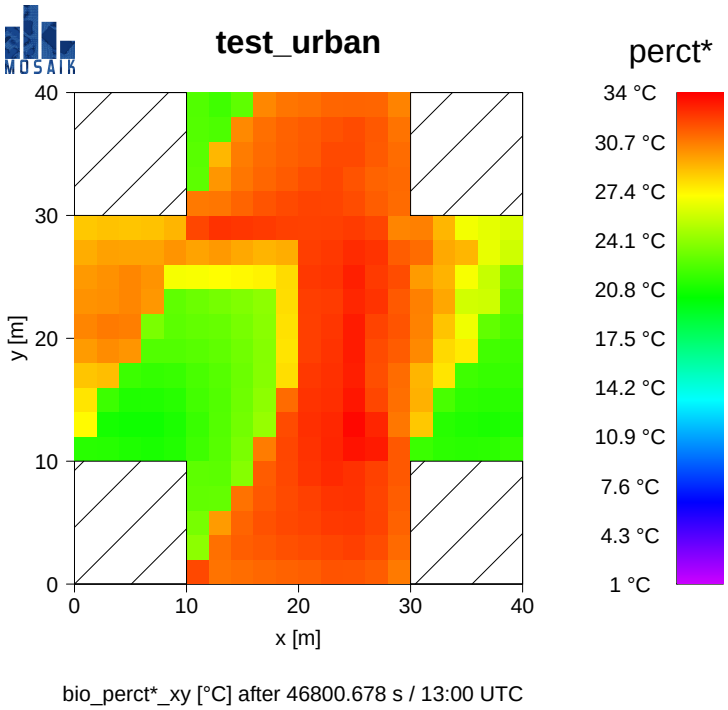

Figure 5. Perceived Temperature (PT, perct* in palm) for the test case "test_urban" at 13:00 UTC (close to midday) on a 6$^{\text{th}}$ of March. Incident wind is from 270° with 1.0 m/s.

Taking a closer look at Figure 6 one can see, that the results for UTCI appear to be more homogeneous in some areas than those for PT (compare to 4). One of those areas can be found in between the buildings on the right with UTCI of 18.1 - 18.3 °C. They are mostly caused by wind speed going below the valid range for wind speed to the UTCI regression equation (see Section 2.1.1).

3.1 Comparison with SkyHelios

A similar model domain was created for the SkyHelios model (Fröhlich and Matzarakis, 2018; Fröhlich, 2017; Matzarakis and Matuschek, 2011) and a run with similar input parameters was performed. Results for the Perceived Temperature (see Figure 7) show overall cooler conditions compared to the results by PALM (compare to Figures 4 and 5).

Comparing the results for 07:00 UTC on a 6$^{\text{th}}$ of March (Figures 4 and 7 (left)) the SkyHelios results generally are looking more homogeneous. This can be explained by air temperature and air humidity are considered static throughout the model domain in this comparison. Also the diagnostic wind model in SkyHelios generates more homogeneous wind fields in the absence of near-by obstacles. However, the results for PT are not only more homogeneous, but also significantly lower as calculated by SkyHelios than those by PALM. PT after SkyHelios ranges from 5.2 °C in the shade to a maximum of 11.4 °C in the sun in areas with very low wind speed (e.g. at the South-Western corner of the upper right building). This is way less

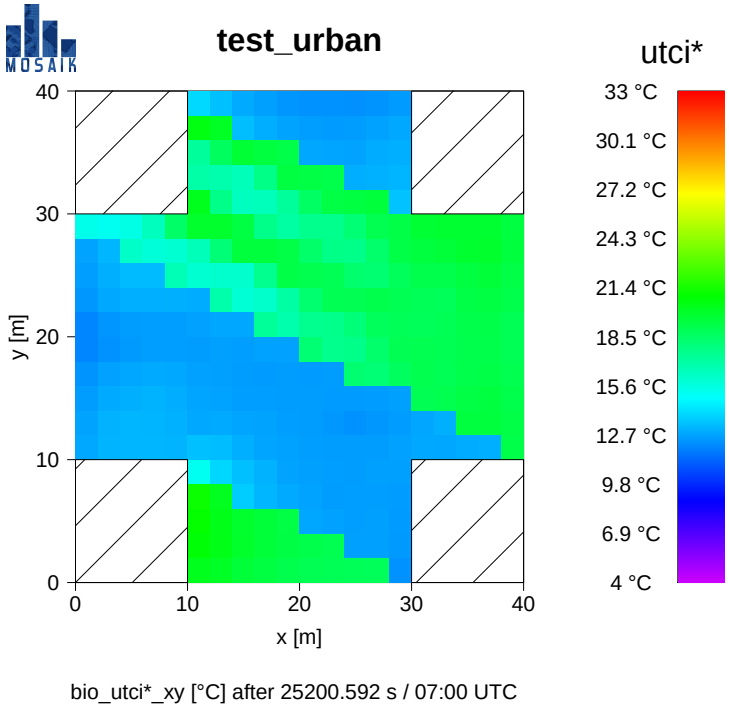

Figure 6. Universal Thermal Climate Index (UTCI, utci* in palm) for the test case "test_urban" at 07:00 UTC (shortly after sunrise) on a 6th of March.

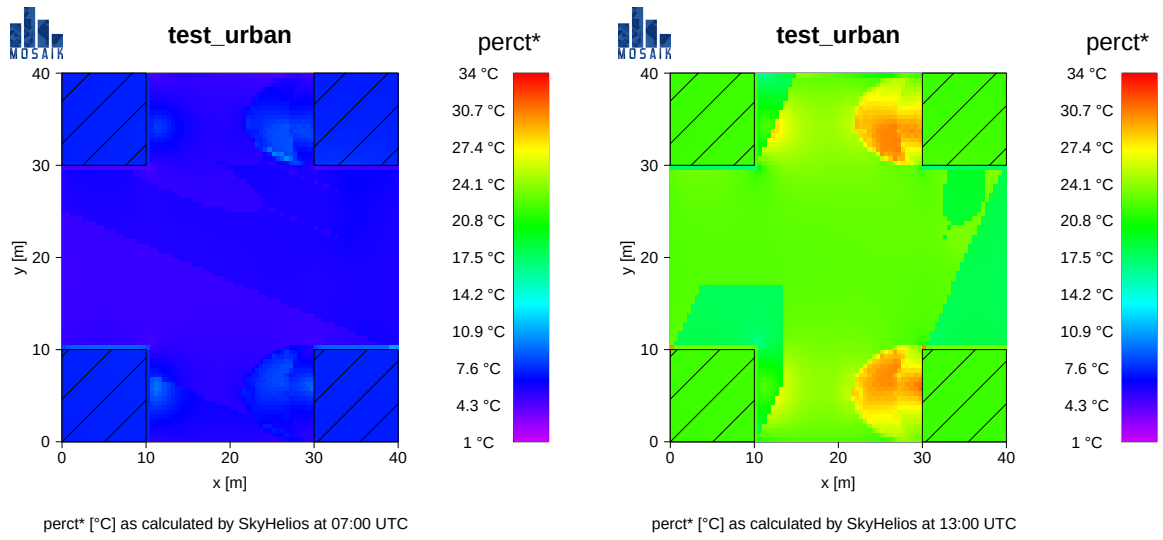

Figure 7. Perceived Temperature (PT, perct* in palm) for the test case "test_urban" at 07:00 UTC (left) and 13:00 UTC (right) on a 6th of March as calculated by the SkyHelios model.

than the PT calculated by PALM ranging from 10.2 to 15.6 °C in the sun and 8.0 to 11.1 °C in shaded areas. For the SkyHelios results, even the 3rd quantile of the PT results at 07:00 UTC of 7.9 °C is lower than the minimum value calculated by PALM. A similar pattern can be found for the PT results at 13:00 UTC. Comparing Figures 4 and 7 (left) one can see once again that the SkyHelios results are more homogeneous for the reasons described above. However, the results calculated by SkyHelios are, again significantly lower than those by PALM. For the time of 13:00 UTC PT calculated by SkyHelios ranges from 16.6 °C in shaded areas to a maximum of 30.5 °C. The latter, however, is only reached in wind sheltered areas (West of the upper and lower right obstacle) that are exposed to direct radiation at the same time. Areas without the wind sheltering effect (e.g. in the central area of the domain) are significantly cooler (around 22.5 °C) even if they are exposed to direct radiation. PALM calculates way higher values of PT of 20.0 - 23.4 °C in the shade and 24.4 - 30.9 °C in the sun (see above).

Both, the differences at 07:00 as well as at 13:00 UTC can be explained by rather strong disagreement in the mean radiant temperature. While SkyHelios estimates mean radiant temperature of 4.7 °C in the shade to a maximum of 14.5 °C in the sun for the 07:00 UTC scenario, the same values are ranging from 11.4 °C to 35.4 °C in PALM. For the 13:00 UTC situation the disagreement is little lower: While SkyHelios does calculate $\mathrm{T_{mrt}}$ of 25.0 °C to 47.5 °C, PALM results in the range of 25.7 °C up to 51.7 °C.

3.2 Comparison to VDI versions and RayMan results

To get an insight on the precision of the results obtained from the biometeorology module, a direct comparison of results by the thermal index programs published in the VDI guideline 3787 (VDI, 2008), as well as by the RayMan model was performed based on the same input data (please refer to Section 2.3 for details). The result for each index calculated by the biometeorology module fore a set of data was substracted by the respective VDI and RayMan version. An overview over the deviations is provided by Table 5.

Table 5. Statistical overview over the comparison of the results generated by the module for the thermal indices PT, PET and UTCI to those by the respective versions published in VDI guideline 3787 (VDI, 2008) and by the RayMan model.

	VDI			RayMan		
	PT	PET	UTCI	PT	PET	UTCI
Min.	-2.094	-0.037	0.000	-2.106	-0.418	-0.070
1st Qu.	-0.003	-0.004	0.000	-0.044	0.019	-0.020
Median	-0.001	0.003	0.000	-0.009	0.052	0.000
Mean	-0.002	0.004	0.000	-0.058	0.054	0.000
3rd Qu.	0.000	0.011	0.000	0.019	0.086	0.030
Max.	1.356	0.083	0.000	2.683	0.488	0.070
NA's	17073	17073	17073	17073	17073	211265

The comparison between the results for PT calculated by the biometeorology module and the VDI version reveils some deviation of up to 2.094 K in rare cases (deviation of 0.1 K or more in 0.027 % of all cases tested in this study). The average deviations are found to be very low (0.002 K).

For the index PET the deviation between the results by the biometeorology module and the VDI version of the index is slightly higher in average (0.004 K) but does never reach a relevant level of 0.1 K (maximum of 0.083 K). Small deviations are to be expected due to rounding errors in the iterative PET calculations.

For UTCI no deviation can be found between the results generated by the biometeorology module and the VDI version of the index at all. This can be explained through UTCI is determined by the regression equation in both cases an, thus, is the least complex index in the comparison (no iterations).

The deviations to the results of the RayMan model are slightly higher for all indices. For PT, the deviation is up to 2.683 K, for PET the maximum deviation is is 0.488 K while there is only a slight deviation of up to 0.07 K for the index UTCI. The higher deviations, however, can easily be explained by RayMan running on lower precision and rounding results to 0.1 K.

4 Discussion and Conclusions

The implementation of the thermal indices PT, UTCI and PET as a part of the newly developed biometeorology module does allow for a quantitative assessment of thermal comfort and thermal stress (e.g. Staiger et al., 2019) using the model PALM-4U (Maronga et al., 2019b). Results show that the human thermal comfort part of the biometeorology module can generate reliable and plausible results for either of the indices in grid resolution for the vertical cell layer closest to 1.1 m above ground level.

The results presented in this study might seem quite high for the date of the case study, the 6^{th} of March. However, with an air temperature ranging from 3.9 °C shortly after midnight to 23.9 °C in the afternoon the values are to be expected in this region. Another reason for the hot conditions is the large radiational gain generated by the "clear-sky" scheme, that causes the mean radiant temperature to rise from -0.1 °C prior to sunrise to a maximum of 52.0 °C in the early afternoon. Furthermore considering the overall low wind speed, hot conditions as presented here are to be expected (e.g. Fröhlich et al., 2019).

Comparing the results calculated by the biometeorology module to those calculated by the SkyHelios model, the ones by SkyHelios appear to be significantly lower. This is, as described above, mostly due to differences in the mean radiant temperature. Also wind speed calculated by SkyHelios for an incident surface wind speed of 1.0 m/s from 270 ° is higher (around 0.1 m/s to 0.9 m/s) than the wind speed calculated by PALM (less than 0.1 m/s to 0.5 m/s at 07:00 UTC).

Both issues might be arising from the grid resolution used in the test calculations. With a grid resolution of 2.0 m on 2.0 m on 2.0 m the grid used for the PALM run is rather coarse. While this is required to keep the computational effort in reasonable scale for a complex model like PALM (Maronga et al., 2015) it decreases precision of the results (Fröhlich and Matzarakis, 2018). This definitely holds for the radiation calculations where the rather coarse obstacles throw stair-like shadows (Fröhlich and Matzarakis, 2018), but also for wind speed in the target height of 1.1 m. As 1.1 m is within the lowest possible layer of cells ground friction might be overestimated in the wind input to the biometeorology module. The SkyHelios model, in contrast, does perform radiation calculations in a vector-based model domain while the lower computational effort allows for higher

target resolutions (Fröhlich and Matzarakis, 2018). To minimize the negative effects of the rasterized calculations in PALM, a high resolution of e.g. 1 m on 1 m horizontally, as well as even higher vertical resolutions (e.g. with telescoping and nesting as proposed by Hellsten et al., 2018) is recommended by the authors.

Considering the same input to the biometeorology module in terms of air temperature, moisture, wind velocity and mean radiant temperature, the output for PT, UTCI and PET does agree very well (considering the usual rounding effects) to reference calculations by the VDI version of the respective index as well as to results by the RayMan model (Matzarakis et al., 2007, 2010).

The new functionality implemented in the biometeorology module is intended to facilitate the consideration of several aspects of human thermal comfort and stress for various applications and user groups. This allows for the replacement of older and potentially less comprehensive models and methods not only in biometeorological research applications (e.g. Reis and Lopes, 2019; Nouri et al., 2018). It can be used by architects and municipalities to analyze the effect o their design on human thermal perception and health (e.g. Conti et al., 2005; Lin et al., 2010b; Fröhlich and Matzarakis, 2013) to improve their concepts e.g. fighting the local effect of global climate change or the urban heat island (Reis and Lopes, 2019).

Code availability. The specific version of PALM applied is provided in the folder SOURCE of Fröhlich (2019). In general, the PALM model system is free software. It can be redistributed and/or modified under the terms of the GNU General Public License (v3). We kindly request that you cite PALM in all your publications. It is available online as described in the PALM installation instructions: https://palm.muk.uni-hannover.de/trac/wiki/doc/install.

Data availability. The modified "test_urban" input dataset along with the results and the respective model source is available online along with Fröhlich (2019). It is a modification of the generic PALM test–case "test_urban" provided at https://palm.muk.uni-hannover.de/mosaik/wiki/internal/testing (last access on 2019-06-19).

Author contributions. conceptualization, Dominik Fröhlich; methodology, Dominik Fröhlich and Andreas Matzarakis; software, Dominik Fröhlich and Andreas Matzarakis; validation, Dominik Fröhlich and Andreas Matzarakis; formal analysis, Dominik Fröhlich and Andreas Matzarakis; investigation, Dominik Fröhlich and Andreas Matzarakis; resources, Andreas Matzarakis, Dominik Fröhlich; data curation, Dominik Fröhlich; writing—original draft preparation, Dominik Fröhlich and Andreas Matzarakis; writing—review and editing, Andreas Matzarakis, Dominik Fröhlich; visualization, Dominik Fröhlich; supervision, Andreas Matzarakis; project administration, Andreas Matzarakis; funding acquisition, Andreas Matzarakis

Competing interests. The authors declare no competing interests.

Acknowledgements. This study is part of the MOSAIK project (https://palm.muk.uni-hannover.de/mosaik, last access December 9, 2019), a part of the $[\mathrm{UC}]^2$ programme (http://www.uc2-program.org/index.php/en?page=structure_partner&lan=en, last access December 9, 2019), and is funded by the German Federal Ministry of Education and Research (BMBF).

References

ASHRAE: Fundamentals. Chapter 8 - Thermal comfort, Tech. rep., American Society of Heating and Air-Conditioning Engineers, Atlanta, 2001.

Bröde, P., Fiala, D., B\lazejczyk, K., Holmér, I., Jendritzky, G., Kampmann, B., Tinz, B., and Havenith, G.: Deriving the operational procedure for the Universal Thermal Climate Index (UTCI), International Journal of Biometeorology, 56, 481–494, https://doi.org/10.1007/s00484-011-0454-1, 2012.

Błażejczyk, K., Epstein, Y., Jendritzky, G., Staiger, H., and Tinz, B.: Comparison of UTCI to selected thermal indices, International Journal of Biometeorology, 56, 515–535, https://doi.org/10.1007/s00484-011-0453-2, wOS:000303461000010, 2012.

Błażejczyk, K., Jendritzky, G., Bröde, P., Fiala, D., Havenith, G., Epstein, Y., Psikuta, A., and Kampmann, B.: An introduction to the Universal Thermal Climate Index (UTCI), Geographia Polonica, 86, 2013.

Charalampopoulos, I., Tsiros, I., Chronopoulou-Sereli, A., and Matzarakis, A.: Analysis of thermal bioclimate in various urban configurations in Athens, Greece, Urban Ecosystems, 16, 217–233, https://doi.org/10.1007/s11252-012-0252-5, wOS:000318444400004, 2013.

Charalampopoulos, I., Tsiros, I., Chronopoulou-Sereli, A., and Matzarakis, A.: A note on the evolution of the daily pattern of thermal comfort-related micrometeorological parameters in small urban sites in Athens, International Journal of Biometeorology, 59, 1223–1236, https://doi.org/10.1007/s00484-014-0934-1, wOS:000359535200009, 2015.

Chen, Y.-C. and Matzarakis, A.: Modified physiologically equivalent temperature—basics and applications for western European climate, Theoretical and Applied Climatology, 132, 1275–1289, https://doi.org/10.1007/s00704-017-2158-x, http://link.springer.com/10.1007/s00704-017-2158-x, 2018.

Conti, S., Meli, P., Minelli, G., Solimini, R., Toccaceli, V., Vichi, M., Beltrano, C., and Perini, L.: Epidemiologic study of mortality during the Summer 2003 heat wave in Italy, Environmental Research, 98, 390–399, https://doi.org/10.1016/j.envres.2004.10.009, wOS:000229724200013, 2005.

Fanger, P.: Thermal comfort, McGraw-Hill, New York, 1972.

Fiala, D., Havenith, G., Broede, P., Kampmann, B., and Jendritzky, G.: UTCI-Fiala multi-node model of human heat transfer and temperature regulation, International Journal of Biometeorology, 56, 429–441, https://doi.org/10.1007/s00484-011-0424-7, wOS:000303461000003, 2012.

Fröhlich: Modified "test_urban" dataset for thermal comfort in PALM, https://doi.org/10.5281/zenodo.3567814, https://doi.org/10.5281/zenodo.3567814, 2019.

Fröhlich, D.: Development of a microscale model for the thermal environment in complex areas, Ph.D. thesis, Albert-Ludwigs-Universität, Freiburg, https://freidok.uni-freiburg.de/data/11614, doi: 10.6094/UNIFR/11614, 2017.

Fröhlich, D. and Matzarakis, A.: Thermal bioclimate and urban planning in Freiburg - Examples based on urban spaces, Theoretical and Applied Climatology, pp. 547–558, 2013.

Fröhlich, D. and Matzarakis, A.: A quantitative sensitivity analysis on the behaviour of common thermal indices under hot and windy conditions in Doha, Qatar, Theoretical and Applied Climatology, 124, 179–187, https://doi.org/10.1007/s00704-015-1410-5, wOS:000373143600014, 2016.

Fröhlich, D. and Matzarakis, A.: Spatial Estimation of Thermal Indices in Urban Areas-Basics of the SkyHelios Model, Atmosphere, 9, 209, https://doi.org/10.3390/atmos9060209, wOS:000436271900007, 2018.

Fröhlich, D., Gangwisch, M., and Matzarakis, A.: Effect of radiation and wind on thermal comfort in urban environments - Application of the RayMan and SkyHelios model, Urban Climate, 27, 1–7, https://doi.org/10.1016/j.uclim.2018.10.006, http://www.sciencedirect.com/science/article/pii/S2212095518303225, 2019.

Gagge, A., Fobelets, A., and Berglund, L.: A standard predictive index of human response to the thermal environment, ASHRAE Transactions, pp. 709–731, 1986.

Havenith, G., Fiala, D., Błazejczyk, K., Richards, M., Bröde, P., Holmér, I., Rintamaki, H., Benshabat, Y., and Jendritzky, G.: The UTCI-clothing model, Int J Biometeorol, 56, 461–470, https://doi.org/10.1007/s00484-011-0451-4, 2012.

Helbig, A., Baumüller, J., and Kerschgens, M. J.: Stadtklima und Luftreinhaltung. 2., vollständig überarbeitete und ergänzte Auflage mit 200 Abbildungen und 79 Tabellen, Springer-Verlag, Berlin; Heidelberg [u.a.], 2 edn., 1999.

Hellsten, A., Ketelsen, K., Barmpas, F., Tsegas, G., Moussiopoulos, N., and Raasch, S.: Nested Multi-scale System in the PALM Large-Eddy Simulation Model, in: Air Pollution Modeling and its Application XXV, edited by Mensink, C. and Kallos, G., pp. 287–292, Springer International Publishing, Cham, https://doi.org/10.1007/978-3-319-57645-9_45, http://link.springer.com/10.1007/978-3-319-57645-9_45, 2018.

Höppe, P.: Die Energiebilanz des Menschen, Berichte des Meteorologischen Instituts Nr. 49, Ludwigs-Maximilians-Universität, München, 1984.

Höppe, P. R.: Heat balance modelling, Experientia, 49, 741–746, http://dx.doi.org/10.1007/BF01923542, 1993.

Höppe, P. R.: The physiological equivalent temperature – a universal index for the biometeorological assessment of the thermal environment, Int J Biometeorol, 43, 71–75, 1999.

Jendritzky, G., Menz, H., Schirmer, H., and Schmidt-Kessen, W.: Methodik zur raumbezogenen Bewertung der thermischen Komponente im Bioklima des Menschen (Fortgeschriebenes Klima- Michel-Modell), Beitr Akad Raumforsch Landesplan, 1990.

Jendritzky, G., de Dear, R., and Havenith, G.: UTCI-Why another thermal index?, Int J Biometeorol, pp. 421–428, 2012.

Koppe, C., Kovats, S., Jendritzky, G., and Menne, B.: Heat-waves: risks and responses, vol. 2, World Health Organization, Copenhagen, 2004.

Lin, T.-P., Matzarakis, A., and Hwang, R.-L.: Shading effect on long-term outdoor thermal comfort, Building and Environment, 45, 213–221, https://doi.org/10.1016/j.buildenv.2009.06.002, 2010a.

Lin, T.-P., Matzarakis, A., Hwang, R.-L., and Huang, Y.-C.: Effect of pavements albedo on long-term outdoor thermal comfort, in: Proceedings of the 7th Conference on Biometeorology, vol. 20 of *Ber. Meteorol. Inst. Univ. Freiburg*, pp. 498–504, Freiburg, 2010b.

Maronga, B., Gryschka, M., Heinze, R., Hoffmann, F., Kanani-Sühring, F., Keck, M., Ketelsen, K., Letzel, M. O., Sühring, M., and Raasch, S.: The Parallelized Large-Eddy Simulation Model (PALM) version 4.0 for atmospheric and oceanic flows: model formulation, recent developments, and future perspectives, Geoscientific Model Development, 8, 2515–2551, https://doi.org/10.5194/gmd-8-2515-2015, https://www.geosci-model-dev.net/8/2515/2015/, 2015.

Maronga, B., Banzhaf, S., Burmeister, C., Esch, T., Forkel, R., Fröhlich, D., Fuka, V., Gehrke, K. F., Geletič, J., Giersch, S., Gronemeier, T., Groß, G., Heldens, W., Hellsten, A., Hoffmann, F., Inagaki, A., Kadasch, E., Kanani-Sühring, F., Ketelsen, K., Khan, B. A., Knigge, C., Knoop, H., Krč, P., Kurppa, M., Maamari, H., Matzarakis, A., Mauder, M., Pallasch, M., Pavlik, D., Pfafferott, J., Resler, J., Rissmann, S., Russo, E., Salim, M., Schrempf, M., Schwenkel, J., Seckmeyer, G., Schubert, S., Sühring, M., von Tils, R., Vollmer, L., Ward, S., Witha, B., Wurps, H., Zeidler, J., and Raasch, S.: Overview of the PALM model system 6.0, https://doi.org/10.5194/gmd-2019-103, https://www.geosci-model-dev-discuss.net/gmd-2019-103/, 2019a.

Maronga, B., Gross, G., Raasch, S., Banzhaf, S., Forkel, R., Heldens, W., Kanani-Sühring, F., Matzarakis, A., Mauder, M., Pavlik, D., Pfafferott, J., Schubert, S., Seckmeyer, G., Sieker, H., and Winderlich, K.: Development of a new urban climate model based on the model PALM – Project overview, planned work, and first achievements, Meteorologische Zeitschrift, 28, 105–119, https://doi.org/10.1127/metz/2019/0909, http://www.schweizerbart.de/papers/metz/detail/28/90483/Development_of_a_new_urban_climate_model_based_on_?af=crossref, 2019b.

Matzarakis, A.: Die thermische Komponente des Stadtklimas, no. 6 in Berichte des Meteorologischen Institutes der Universität Freiburg, 2001.

Matzarakis, A. and Endler, C.: Climate change and thermal bioclimate in cities: impacts and options for adaptation in Freiburg, Germany, Int J Biometeorol, 54, 479–483, https://doi.org/10.1007/s00484-009-0296-2, http://dx.doi.org/10.1007/s00484-009-0296-2, 2010.

Matzarakis, A. and Matuschek, O.: Sky view factor as a parameter in applied climatology rapid estimation by the SkyHelios model, Meteorologische Zeitschrift, 20, 39–45, 2011.

Matzarakis, A. and Mayer, H.: Another kind of environmental stress: Thermal stress, WHO Newsletter, pp. 7–10, 1996.

Matzarakis, A., Rutz, F., and Mayer, H.: Modelling radiation fluxes in simple and complex environments - application of the RayMan model, Int. J. Biometeorol., 51, 323–334, https://doi.org/10.1007/s00484-006-0061-8, wOS:000244681400008, 2007.

Matzarakis, A., Rutz, F., and Mayer, H.: Modelling radiation fluxes in simple and complex environments: basics of the RayMan model, Int. J. Biometeorol., 54, 131–139, https://doi.org/10.1007/s00484-009-0261-0, wOS:000274903900003, 2010.

Mayer, H. and Höppe, P.: Thermal Comfort of Man in Different Urban Environments, Theoretical and Applied Climatology, pp. 43–49, 1987.

Mlawer, E., Taubman, S., Brown, P., Iacono, M., and Clough, S.: RRTM, a validated correlated-k model for the longwave, J. Geophys. Res., 16, 663–682, 1997.

Muthers, S., Matzarakis, A., and Koch, E.: Summer climate and mortality in Vienna - a human-biometeorological approach of heat-related mortality during the heat waves in 2003, Wiener Klinische Wochenschrift, 122, 525–531, https://doi.org/10.1007/s00508-010-1424-z, wOS:000282225200002, 2010.

Muthers, S., Laschewski, G., and Matzarakis, A.: The Summers 2003 and 2015 in South-West Germany: Heat Waves and Heat-Related Mortality in the Context of Climate Change, Atmosphere, 8, 224, https://doi.org/10.3390/atmos8110224, http://www.mdpi.com/2073-4433/8/11/224, 2017.

Nastos, P. and Matzarakis, A.: The effect of air temperature and Physiologically Equivalent Temperature on mortality in Athens, Greece, Theoretical and Applied Climatology, pp. 591–599, 2012.

Nouri, A. S., Fröhlich, D., Silva, M. M., and Matzarakis, A.: The Impact of Tipuana tipu Species on Local Human Thermal Comfort Thresholds in Different Urban Canyon Cases in Mediterranean Climates: Lisbon, Portugal, Atmosphere, 9, https://doi.org/10.3390/atmos9010012, http://www.mdpi.com/2073-4433/9/1/12, 2018.

Oke, T. R.: Boundary layer climates, 2nd edition, Routledge, London, New York, 1995.

Pincus, R., Barker, H. W., and Morcrette, J.-J.: A fast, flexible, approximate technique for computing radiative transfer in inhomogeneous cloud fields: FAST, FLEXIBLE, APPROXIMATE RADIATIVE TRANSFER, Journal of Geophysical Research: Atmospheres, 108, n/a–n/a, https://doi.org/10.1029/2002JD003322, http://doi.wiley.com/10.1029/2002JD003322, 2003.

Raasch, S. and Schröter, M.: PALM - A large-eddy simulation model performing on massively parallel computers, Meteorologische Zeitschrift, 10, 363–372, https://doi.org/10.1127/0941-2948/2001/0010-0363, http://www.schweizerbart.de/papers/metz/detail/10/49174/PALM_A_large_eddy_simulation_model_performing_on_m?af=crossref, 2001.

Reis, C. and Lopes, A.: Evaluating the Cooling Potential of Urban Green Spaces to Tackle Urban Climate Change in Lisbon, Sustainability, 11, 2480, https://doi.org/10.3390/su11092480, https://www.mdpi.com/2071-1050/11/9/2480, 2019.

Resler, J., Krč, P., Belda, M., Juruš, P., Benešová, N., Lopata, J., Vlček, O., Damašková, D., Eben, K., Derbek, P., Maronga, B., and Kanani-Sühring, F.: PALM-USM v1.0: A new urban surface model integrated into the PALM large-eddy simulation model, Geoscientific Model Development, 10, 3635–3659, https://doi.org/10.5194/gmd-10-3635-2017, https://www.geosci-model-dev.net/10/3635/2017/, 2017.

Shashua-Bar, L., Pearlmutter, D., and Erell, E.: The influence of trees and grass on outdoor thermal comfort in a hot-arid environment, International Journal of Climatology, 31, 1498–1506, https://doi.org/10.1002/joc.2177, wOS:000293247600007, 2011.

Staiger, H., Laschewski, G., and Graetz, A.: The perceived temperature - a versatile index for the assessment of the human thermal environment. Part A: scientific basics, International Journal of Biometeorology, 56, 165–176, https://doi.org/10.1007/s00484-011-0409-6, wOS:000298393800017, 2012.

Staiger, H., Laschewski, G., and Matzarakis, A.: Selection of Appropriate Thermal Indices for Applications in Human Biometeorological Studies, Atmosphere, 10, 18, https://doi.org/10.3390/atmos10010018, https://www.mdpi.com/2073-4433/10/1/18, 2019.

Tromp, S.: Biometeorology. The impact of the weather and climate on humans and their environment (animals and plants), Heyden & Son Ltd, London, Philadelphia, Rheine, 1980.

VDI: VDI Guideline 3787, Part 2: Environmental Meteorology. Methods for the human biometeorological evaluation of climate and air quality for urban and regional planning at regional level. Part I: Climate, Tech. Rep. 1b, VDI, 2008.